Oxidative Modifications Switch Modulatory Activities of Urinary Proteins From Inhibiting to Promoting Calcium Oxalate Crystallization, Growth, and Aggregation

Authors

Sakdithep Chaiyarit, and Visith Thongboonkerd

Correspondence

thongboonkerd@dr.com;
vthongbo@yahoo.com

In Brief

Previous evidence has shown that oxidative stress commonly occurs in kidney stone disease. But all the references have indicated the occurrence of oxidative stress (as the result or complication) after the stone or disease has been already developed. However, its etiologic role (as the cause) remains unknown. This first piece of evidence highlights the essential role of oxidative modifications of urinary proteins as one of the etiologies causing kidney stone formation.

Graphical Abstract

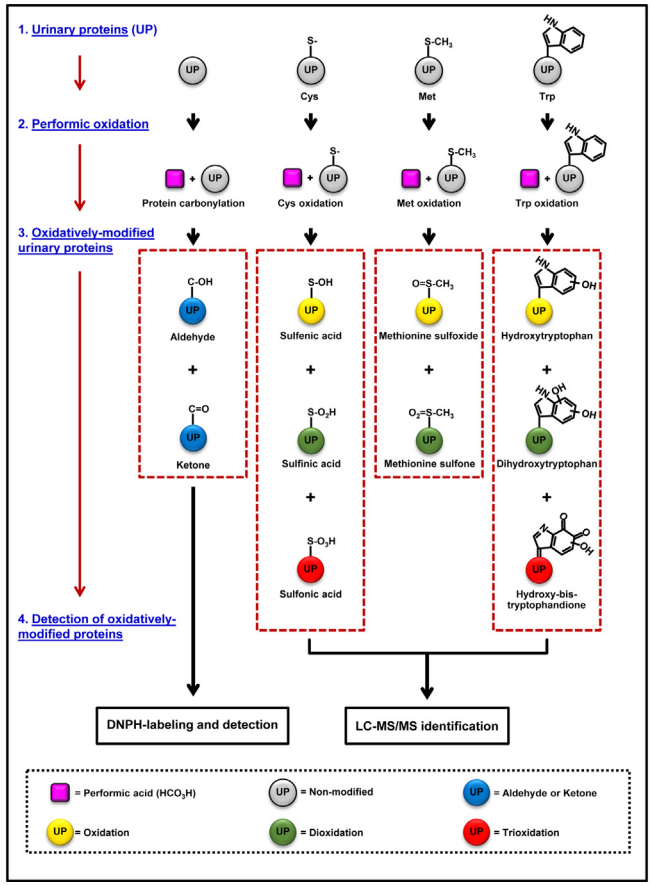

Highlights

- About 1121 of 5297 oxidized peptides were found in nonmodified/modified urine.
- Oxyblot confirms successful oxidation of urinary proteins by performic acid.
- Nonmodified urinary proteins inhibit crystallization, crystal growth/aggregation.
- Oxidized urinary proteins promote crystallization, crystal growth, and aggregation.

2021, Mol Cell Proteomics *20*, 100151

https://doi.org/10.1016/j.mcpro.2021.100151

Oxidative Modifications Switch Modulatory Activities of Urinary Proteins From Inhibiting to Promoting Calcium Oxalate Crystallization, Growth, and Aggregation

Sakdithep Chaiyarit and Visith Thongboonkerd*

The incidence/prevalence of kidney stone disease has been increasing around the globe, but its pathogenic mechanisms remained unclear. We evaluated effects of oxidative modifications of urinary proteins on calcium oxalate (CaOx) stone formation processes. Urinary proteins derived from 20 healthy individuals were modified by performic oxidation, and the presence of oxidatively modified urinary proteins was verified, quantified, and characterized by Oxyblot assay and tandem MS (nanoLC–electrospray ionization–linear trap quadrupole-Orbitrap–MS/MS). Subsequently, activities of oxidatively modified urinary proteins on CaOx stone formation processes were examined. Oxyblot assay confirmed the marked increase in protein oxidation level in the modified urine. NanoLC–electrospray ionization–linear trap quadrupole-Orbitrap–MS/MS identified a total of 193 and 220 urinary proteins in nonmodified and modified urine samples, respectively. Among these, there were 1121 and 5297 unambiguous oxidatively modified peptides representing 42 and 136 oxidatively modified proteins in the nonmodified and modified urine samples, respectively. Crystal assays revealed that oxidatively modified urinary proteins significantly promoted CaOx crystallization, crystal growth, and aggregation. By contrast, the nonmodified urinary proteins had inhibitory activities. This is the first direct evidence demonstrating that oxidative modifications of urinary proteins increase the risk of kidney stone disease by switching their modulatory activities from inhibiting to promoting CaOx crystallization, crystal growth, and aggregation.

Despite enormous efforts in studying kidney stone disease, its incidence/prevalence has been increasing around the globe (1, 2). Crystal nucleation (crystallization), growth, aggregation, and adhesion on renal tubular cells have been proposed as the important mechanisms for kidney stone formation (1, 2). Thus, findings of the pivotal factors regulating these stone formation steps are motivated to define the effective prevention strategies. Involvements of urinary proteins, such as uromodulin (3), uropontin (4), albumin (5, 6), nephrocalcin (7), prothrombin fragment 1 (8), bikunin (9–11), trefoil factor 1 (12, 13), and fibronectin (14), in modulation of nucleation, growth, aggregation, and adhesion of calcium oxalate (CaOx) crystals (the major composition of kidney stones) have been revealed in previous studies. However, the precise roles of these proteins in the stone pathogenesis remain unclear.

Interestingly, clinical and animal studies have demonstrated the increasing evidence of oxidative stress in kidney stone disease (15–19). Likewise, recent findings have shown that the interactions between CaOx crystals and renal tubular cells can promote many cellular events, such as cell proliferation (20), cell death (21), cellular injury (22), mitochondrial dysfunction (23), and inflammatory cascade (24). All these cellular events are associated with oxidative stress and overproduction of free radicals and reactive oxygen species (ROS) such as superoxide and hydrogen peroxide (H_2O_2) in renal tubular cells (25). However, almost all these references have shown that oxidative stress is a secondary event following the stone development, crystal deposition, or exposure to the known etiologic factors (*i.e.*, hyperoxaluria, hypercalciuria) (15–27), whereas its primary role as the etiology remains unclear.

Interestingly, extracellular ROS are also found in the urinary system (28). ROS, also known as DNA-damage agents, can change protein functions and properties by oxidization at free thiol group of cysteine and are associated with many diseases (29–31). Oxidation of these thiol groups (sulfoxidation) by superoxide ($O^{2\bullet-}$) and H_2O_2 can generate reversible sulfenic acid (–SOH). Under severe oxidizing condition, high level of ROS can modify sulfenic acid to the irreversible sulfinic ($–SO_2H$) and sulfonic ($–SO_3H$) acid (32). Consequently, extracellular ROS can modify urinary proteins, lipids, and nucleic acids,

From the Medical Proteomics Unit, Office for Research and Development, Faculty of Medicine Siriraj Hospital, Mahidol University, Bangkok, Thailand

*For correspondence: Visith Thongboonkerd, thongboonkerd@dr.com or vthongbo@yahoo.com.

https://doi.org/10.1016/j.mcpro.2021.100151

resulting to alterations of their functional activities. Urinary and crystal-associated proteins are known to get involved in kidney stone formation (33–35). We then hypothesized that oxidative modifications of urinary proteins may be one of the key factors that promote kidney stone formation. Therefore, this study aimed to examine the roles for oxidatively modified urinary proteins in kidney stone formation processes.

EXPERIMENTAL PROCEDURES

Urine Collection and Sample Preparation

The experiments involving human subjects and clinical samples in this study were approved by the Siriraj Institutional Review Board, Human Research Protection Unit, Faculty of Medicine Siriraj Hospital, Mahidol University, Thailand (ethical approval no.: Si473/2015). All the experiments were conducted according to the international guidelines, that is, the Declaration of Helsinki, the Belmont Report, and ICH Good Clinical Practice, and informed consents were obtained from all subjects.

A total of 100 ml of midstream random urine samples were collected from each of 20 healthy individuals (aged 20–40 years) who had no recent medication or illness. All urine samples were immediately subjected to low-speed centrifugation (1000*g* for 15 min) to remove cell debris and particulate matters. The samples were dialyzed against deionized (18 MΩ cm) water at 4 °C overnight and then lyophilized.

Performic Oxidation of Urinary Proteins

The lyophilized urinary proteins were combined and made into three different pools. Each of these pools were divided into two fractions (nonmodified and modified). For the modified group, the samples were resuspended with formic acid (Thermo Fisher Scientific) to make the final protein concentration at 1 μg/μl, and 3× volume of freshly prepared performic acid (1:20 v/v of 30% H_2O_2 [Thermo Fisher Scientific] in formic acid) was added. After 3-h incubation on ice, 5× volume of ice-cold deionized water was added and then lyophilized. The powder of oxidatively modified proteins was collected and subjected to subsequent experiments.

Oxyblot Analysis

To verify the oxidative modifications in urinary proteins after performic induction, Oxyblot analysis was performed using OxyBlot Protein Oxidation Detection Kit (S7150) (Chemicon) as described previously (36, 37). Briefly, the lyophilized urinary proteins were resuspended in Laemmli's buffer with additional 4% SDS. The proteins were then derivatized with or without 2,4-dinitrophenylhydrazine. Equal amount of the derivatized and nonderivatized urinary proteins (20 μg/sample) were resolved by SDS-PAGE and then transferred onto a nitrocellulose membrane. Thereafter, the membrane was incubated with rabbit polyclonal antidinitrophenyl antibody (Chemicon) (1:500 in 1% bovine serum albumin/PBS) at 25 °C for 1 h, and then with corresponding secondary antibody conjugated with horseradish peroxidase (Dako) (1:1000 in 1% bovine serum albumin/PBS) at 25 °C for 1 h. Finally, the oxidatively modified proteins were detected by SuperSignal West Pico chemiluminescence substrate (Pierce Biotechnology). Band intensity data were obtained using ImageQuant TL software (GE Healthcare).

In-solution Tryptic Digestion by Filter-aided Sample Preparation Method

An equal amount of 50 μg of proteins from modified or nonmodified urine samples was tryptic digested into peptides according to the filter-aided sample preparation protocol as described previously (38, 39). Briefly, protein samples were resuspended in 4% SDS, 100 mM DTT, and 100 mM Tris–HCl (pH 7.6) lysis buffer and were reduced by heating at 95 °C for 5 min. After cooling down at 25 °C, each protein sample was transferred to an Omega Nanosep 10K device (Pall Corporation), added with 200 μl of 8 M urea in 100 mM Tris–HCl (pH 8.5), and then centrifuged at 14,000*g* and 25 °C for 15 min. This buffer exchange step was repeated for one more cycle. The recovered proteins were then alkylated with 100 μl of 50 mM iodoacetamide in 8 M urea/100 mM Tris–HCl (pH 8.5) at 25 °C in the dark using a ThermoMixer C (Eppendorf) for 20 min. Thereafter, buffer exchange was performed twice by centrifugation at 14,000*g* and 25 °C for 15 min each using 200 μl of 8 M urea/100 mM Tris–HCl (pH 8.5). The proteins were then finally exchanged into 50 mM NH_4HCO_3 and digested with sequencing-grade modified trypsin (Promega) in 50 mM NH_4HCO_3 at a ratio of 1:50 (w/w) trypsin/protein at 37 °C for 16 to 18 h in a ThermoMixer C. The digested peptides were collected by transferring the filter unit to a new collection tube and centrifuged at 14,000*g* and 25 °C for 10 to 20 min. Trypsin activity was then stopped by adding 10 μl of 5% formic acid in 80% acetronitrile, and the digested peptides were dried by a SpeedVac concentrator (Savant). The peptides were finally resuspended in 0.1% formic acid prior to MS/MS analysis.

Identification of Oxidatively Modified Urinary Proteins by nanoLC–Electrospray Ionization–Linear Trap Quadrupole-Orbitrap–MS/MS Analysis

Separation of the digested peptides was performed using EASY-nLC II (Thermo Fisher Scientific). Briefly, peptides were loaded from a cooled (7 °C) autosampler into an in-house, 3-cm-long precolumn containing 5-μm C18 resin (Dr Maisch GmbH) and then to an in-house, 15-cm-long analytical column packed with 3-μm C18 resin (Dr Maisch GmbH) using mobile phase A (0.1% formic acid). The peptides were then separated by mobile phase B (acetronitrile/0.1% formic acid) gradient elution with four steps as follows: 2 to 9% for 15 min, 9 to 35% for 85 min, 35 to 95% for 20 min, and then 95% for 10 min at a flow rate of 200 nl/min. Peptide sequences were then analyzed by linear trap quadrupole (LTQ)-Orbitrap-XL (Thermo Fisher Scientific) in positive mode with electrospray ionization (ESI) nanosprayer ion source.

Data were acquired in a collision-induced dissociation top-12 mode under the control of the Xcalibur 2.1.0 and LTQ Tune Plus 2.5.5 software (Thermo Fisher Scientific). The cycle of one full scan was performed at a resolution of 30,000 (300–2000 *m/z*) in the Orbitrap followed by 12 data-dependent MS/MS scans in the linear ion trap with enabled preview mode for FTMS master scan. The minimum signal threshold at 1×10^5 was required for a precursor ion to be selected for further fragmentation. Accumulation target values of full MS and MS/MS scan were 5×10^5 and 3×10^4 ions, respectively. Singly charged ions and unassigned charge states were excluded for fragmentation. Helium was used as a collision gas, and the normalized collision energy was set at 35%. The activation time was 30 ms for acquiring mass spectra. The duration of dynamic exclusion was 180 s.

The MS/MS raw spectra were deconvoluted and then extracted into output searchable.mgf files using Proteome Discoverer, version 1.4.1.14 software (Thermo Fisher Scientific). Mascot software, version 2.4.0 (Matrix Science) was used to search MS/MS spectra against 20,395 entries of human Swiss-Prot database (release 2021_02 on February 7, 2021) with the following standard Mascot parameters for collision-induced dissociation: Enzyme = trypsin, maximal number of missed cleavages = 1, peptide tolerance = ±2 ppm, MS/MS tolerance = ±0.2 Da, fixed modification = carbamidomethyl (C), variable modifications = oxidation (M, C, W), dioxidation (M, C, W) and trioxidation (C, W), charge states = 2+ and 3+, and decoy database on false discovery rate <1%.

In addition, the MS raw files were analyzed by integrated MaxQuant software suite, version 1.5.3.30 (www.maxquant.org) to acquire extracted ion chromatograms and relative spectral intensity for calculating the proportion of peptides containing individual oxidized residues. The derived peak list files were search against the human Swiss-Prot database using built-in Andromeda search engine, which was integrated into MaxQuant software. Fixed modification was carbamidomethylation at cysteine residues, whereas variable modifications were oxidation at methionine, cysteine, or tryptophan, dioxidation at methionine, cysteine, or tryptophan, and trioxidation at cysteine or tryptophan residues. Enzyme specified was trypsin, and only one missed cleavage per peptide was allowed. Data searches were performed with a precursor tolerance of 4.5 ppm and fragmentation tolerance of 0.5 Da with +2 and +3 charge state. The false discovery rate was performed by searching the decoy database and adjusted to 1% at protein level.

Moreover, the unique oxidatively modified peptides were classified as the "unambiguous" oxidatively modified peptides, whereas those that shared peptide sequences with other proteins were considered as the "ambiguous" oxidatively modified peptides. Only the "unambiguous" ones were counted and compared between the nonmodified and modified urine samples.

Effects of Oxidatively Modified Urinary Proteins on CaOx Crystallization

The lyophilized nonmodified and modified urinary proteins were resuspended in the artificial urine (containing 200 mM urea, 1 mM uric acid, 4 mM creatinine, 5 mM $Na_3C_6H_5O_7{\cdot}2H_2O$, 54 mM NaCl, 30 mM KCl, 15 mM NH_4Cl, 3 mM $CaCl_2{\cdot}2H_2O$, 2 mM $MgSO_4{\cdot}7H_2O$, 2 mM $NaHCO_3$, 0.1 mM NaC_2O_4, 9 mM Na_2SO_4, 3.6 mM $NaH_2PO_4{\cdot}H_2O$, and 0.4 mM Na_2HPO_4; pH = 6.2; specific gravity = 1.010 g/ml; and osmolality = 446 mOsm/kg as previously described) (40, 41). Their concentrations were adjusted to 1 μg/μl using the artificial urine. CaOx crystallization was performed as described previously (13, 42). Briefly, 0.5 ml of 10 mM $CaCl_2{\cdot}2H_2O$ in a crystallization buffer containing 10 mM Tris–HCl and 90 mM NaCl (pH 7.4) was added into each well of the 24-well plate (Corning, Inc). An equal volume (4 μl) of proteins (1 μg/μl) derived from each sample was added into each well, whereas 4 μl of the artificial urine (diluent) was added into another well and served as the control. Thereafter, 0.5 ml of 1.0 mM $Na_2C_2O_4$ in the same crystallization buffer was added into each well to make final concentrations of $CaCl_2$ and $Na_2C_2O_4$ at 5 and 0.5 mM, respectively. The mixture was incubated at 25 °C for 1 h. Crystal images were captured randomly from at least 15 high-power fields (HPFs) under Nikon Eclipse Ti-S inverted phase-contrast light microscope (Nikon). Crystal size was measured using NIS Element D software, version 4.11 (Nikon), whereas crystal mass was calculated from at least 100 crystals from 15 HPFs per well using the following equation:

$$\text{Crystal mass}\left(\mu m^2 \,/\, \text{HPF}\right) = \text{Average crystal area in each field}\left(\mu m^2\right) \times \text{Number of crystals in each field}(/\text{HPF}) \quad (1)$$

Effects of Oxidatively Modified Urinary Proteins on CaOx Crystal Growth

CaOx crystal growth assay was performed as described previously (43, 44). Briefly, CaOx crystals were generated in each well of the 24-well plate (Corning, Inc) as described for the crystallization assay. After crystallization was complete (T_0) (at 1 h after mixing $CaCl_2$ with $Na_2C_2O_4$ to exclude an effect from neocrystallization), 4 μl of the artificial urine (control) or the tested proteins (1 μg/μl in the artificial urine) was added into each well. The mixture was further incubated for 60 min (T_{60}). At T_0 and T_{60}, crystal images were captured randomly from at least 15 HPFs per well under the Eclipse Ti-S inverted phase-contrast light microscope. Crystal sizes at T_0 and T_{60} were measured using NIS Element D software, version 4.11 (Nikon), and crystal growth (represented by Δ Crystal area) was calculated from at least 100 crystals in 15 HPFs per well using the following equation:

$$\Delta\text{Crystal area}\left(\mu m^2\right) = \text{Crystal area at } T_{60}\left(\mu m^2\right) - \text{Crystal area at } T_0\left(\mu m^2\right) \quad (2)$$

In addition, crystal growth was evaluated using an oxalate depletion assay as described previously (12, 45). Briefly, the solution in each well derived from the crystal growth assay as described previously was taken at T_0 and T_{60}, and the amount of free oxalate ions was measured by UV spectrophotometry at λ214 nm. Crystal growth (represented by oxalate consumption) and inhibitory activity of modified *versus* nonmodified urinary proteins were calculated using the following equations:

$$\begin{aligned}\text{Oxalate consumption(AU)} = {} & \text{Absorbance}_{(\lambda 214\ \text{nm})} \text{ at } T_0 \\ & - \text{Absorbance}_{(\lambda 214\ \text{nm})} \text{ at } T_{60}\end{aligned} \quad (3)$$

$$\text{Inhibitory activity}(\%) = [(C - T) \,/\, C] \times 100 \quad (4)$$

where C = oxalate consumption without any proteins; T = oxalate consumption with the tested proteins (nonmodified or oxidatively modified urinary proteins).

Note that the negative value of inhibitory activity indicates the promoting activity of the tested protein(s).

Effects of Oxidatively Modified Urinary Proteins on CaOx Crystal Aggregation

CaOx crystal aggregation assay was performed as previously described (46, 47). Briefly, CaOx crystals were generated as described for the crystallization assay but with larger volume. The supernatant was discarded by a centrifugation at 2000*g* for 5 min, whereas CaOx crystals were washed three times with methanol. After another centrifugation at 2000*g* for 5 min, methanol was discarded and the crystals were air dried overnight at 25 °C. CaOx crystals (dry weight of 1000 μg) were resuspended in 1 ml of the crystallization buffer in each well of the 6-well plate (Corning, Inc). An equal volume (4 μl) of the artificial urine (control) or the tested proteins (1 μg/μl in the artificial urine) was added into each well, and the plate was continuously shaken in a shaking incubator (Zhicheng) at 150 rpm and 25 °C for 1 h. Thereafter, formation of CaOx crystal aggregate (defined as an assembly of three or more individual CaOx crystals that tightly joined together) (46, 47) was observed and imaged under the Eclipse Ti-S inverted phase-contrast light microscope. Number of CaOx crystal aggregates was counted from 15 randomized HPFs per well.

Experimental Design and Statistical Rationale

A total of three different pools of urine samples collected from 20 healthy individuals were made, and each pool was divided into two

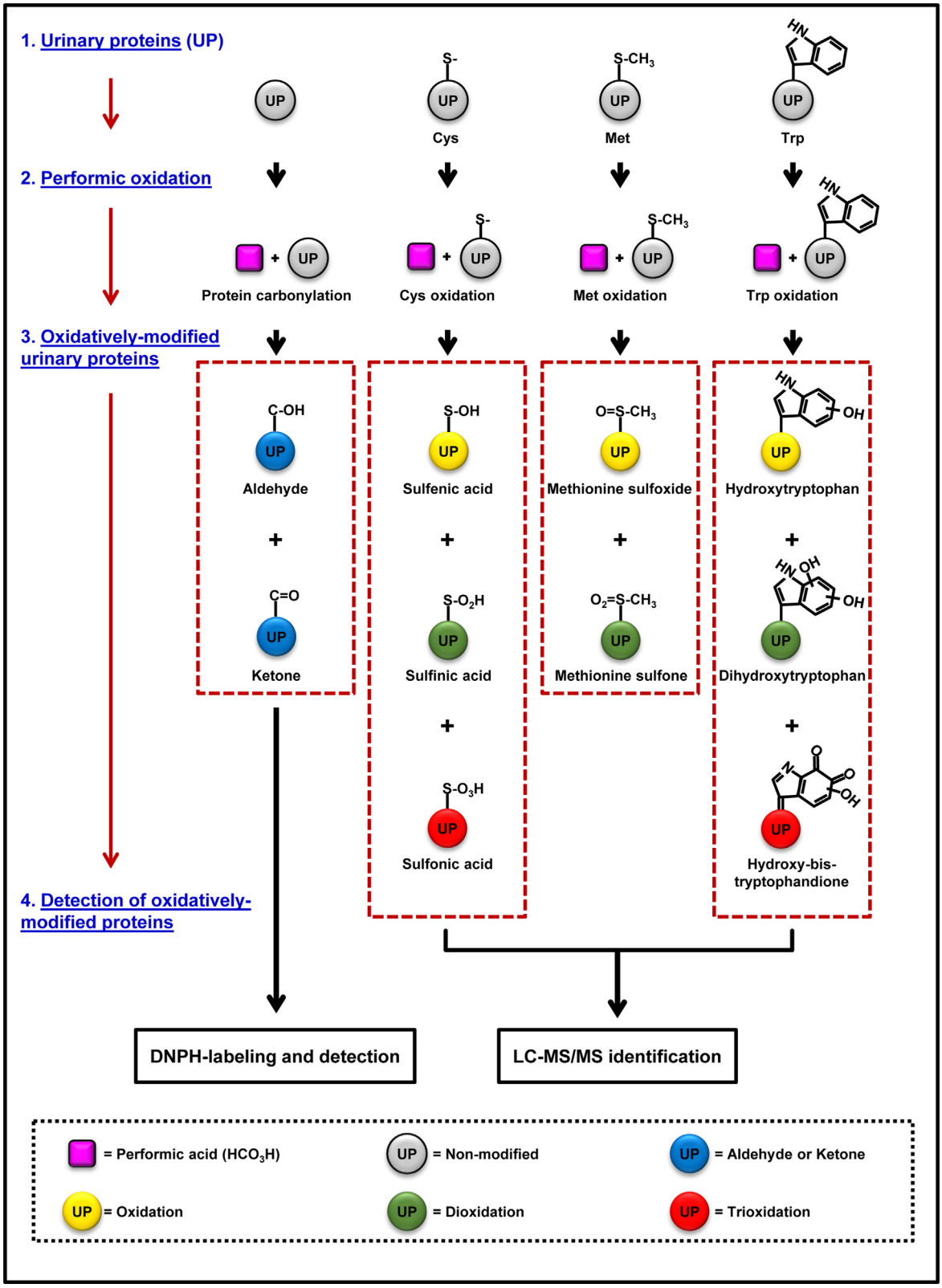

FIG. 1. **Schematic summary for performic oxidation of urinary proteins, products, and detection methods.** A total of three pools of urine samples collected from 20 healthy individuals were made, and each pool was divided into two fractions (nonmodified and modified). For the modified fraction, each of the urine pools was chemically modified by performic acid, which could add carbonyl groups to the proteins and/or oxidize methionine (Met), cysteine (Cys), and/or tryptophan (Trp) residues. The proteins with carbonyl groups (reactive aldehyde and ketone)

fractions (nonmodified and modified). For mass spectrometric analyses and all crystal assays, all these biological replicates were analyzed independently. All quantitative data are reported as mean ± SD unless stated otherwise. Statistical analyses were achieved using SPSS software, version 18.0 (IBM SPSS). Comparisons between two sets of data were performed by unpaired Student's *t* test, whereas multiple comparisons were performed using one-way ANOVA with Tukey's post hoc test. *p* Values less than 0.05 were considered statistically significant.

RESULTS

Our present study aimed to address the involvements of oxidatively modified urinary proteins in kidney stone formation processes. The oxidatively modified urinary proteins were generated and verified as summarized in Figure 1. Oxidative modifications by introducing carbonyl groups as specific side chains and oxidation at methionine (M), cysteine (C), or tryptophan (W) residues were examined by Oxyblot assay and LC–MS/MS analyses, respectively. Oxyblot assay confirmed the marked increase in protein oxidation level in the modified urine obtained from 20 healthy individuals (Fig. 2*A*). NanoLC–ESI–LTQ-Orbitrap–MS/MS identified a total of 193 and 220 urinary proteins in nonmodified and modified urine samples, respectively (supplemental Tables S1–S4). The proteins that were identified with only one peptide were detailed in supplemental Tables S2 and S4. Among all these identified proteins, there were 1121 and 5297 unambiguous oxidatively modified peptides representing 42 and 136 oxidatively modified proteins in the nonmodified and modified urine samples, respectively (supplemental Tables S5 and S6). Also, there were some ambiguous oxidatively modified peptides found in both nonmodified and modified urine samples (supplemental Tables S7 and S8). But only the unambiguous oxidatively modified peptides were counted and compared.

At the protein level, focusing on the significantly identified peptides (with significant MS/MS identification scores), the data showed a marked increase (approximately fivefold) in percentage of oxidatively modified proteins found in the performic-modified urine samples (41.90 ± 1.22%) as compared with the nonmodified ones (8.17 ± 2.38%) (Fig. 2*B*). At the peptide level, when all the peptides were taken into account regardless of their MS/MS identification scores, peptides with dioxidation and those with trioxidation were found in all the modified samples, accounting for 14 to 18% and 16 to 23%, respectively, of all the unambiguous peptides identified, whereas only 1 to 2% of them were found in just one biological replicate of the nonmodified samples (Fig. 2*C* and Table 1).

To obtain more precise quantitative data, the relative spectral intensities of all the oxidatively modified peptides were analyzed based on the extracted ion chromatograms. The quantitative analysis revealed that the percentage of oxidatively modified peptides markedly increased (approximately fourfold) in the modified urine samples compared with the nonmodified samples (Fig. 3*A*). The data on dioxidation and trioxidation were consistent with those of peptide count shown in Figure 2*C*. The data also showed that C (48–51%) and M (33%) were the two most common oxidized residues found in both oxidized and nonoxidized samples, whereas the oxidized W accounted only for 16 to 19% of all the oxidized residues (Fig. 3*B*). Examples of the annotated MS2 spectra of fragmented ions pattern consistent with oxidation (sulfenic acid at C, methionine sulfoxide at M, and hydroxytryptophan at W), dioxidation (sulfinic acid at C, methionine sulfone at M, and dihydroxytryptophan at W), and trioxidation (sulfonic acid at C and hydroxy-bis-tryptophandione at W) are illustrated in Figure 4, *A*–*C*, respectively.

In addition, alterations in the MS chromatogram were observed in the modified urinary proteins with differential pattern of relative abundance and retention time when compared with those of the nonmodified urinary proteins (Fig. 5*A*). Moreover, distribution analysis using Proteome Discoverer revealed that the average molecular mass of the proteins identified from the modified urine (70.73 kDa) was greater than that of the nonmodified urine (63.08), whereas their isoelectric point remained comparable (Fig. 5*B*). All the data obtained from Oxyblot assay and various different approaches by nanoLC–ESI–LTQ-Orbitrap–MS/MS were consistent, confirming that performic acid successfully oxidized the urinary proteins.

CaOx crystallization, growth, and aggregation assays were performed to explore the modulatory effects of oxidatively modified urinary proteins on kidney stone formation processes. As expected, the nonmodified urinary proteins had inhibitory effects against CaOx crystallization (as shown by significant decreases in crystal number, size, and mass) (Fig. 6), crystal growth (as shown by significant decreases in Δ crystal area and oxalate consumption as well as crystal inhibitory activity) (Fig. 7), and crystal aggregation (as shown by significant reduction in number of crystal aggregates) (Fig. 8). By contrast, the oxidatively modified urinary proteins had promoting effects on CaOx crystallization (as shown by significant increases in crystal number, size, and mass) (Fig. 6), crystal growth (as shown by significant increases in Δ crystal area and oxalate consumption, crystal-promoting activity reflecting by the negative inhibitory activity) (Fig. 7), and crystal aggregation (as shown by significant increase in number of crystal aggregates) (Fig. 8).

were detected by 2,4-dinitrophenylhydrazine (DNPH)-derivatized carbonyl immunodetection (Oxyblot assay), whereas the Cys, Met, and Trp oxidation products such as sulfenic (Cys-SOH), sulfinic (Cys-SO_2H), sulfonic (Cys-SO_3H), methionine sulfoxide (Met-SO), methionine sulfone (Met-SO_2), hydroxytryptophan, dihydroxytryptophan, and hydroxy-bis-tryptophandione were identified by nanoLC–ESI–LTQ-Orbitrap–MS/MS analyses. *Gray* = nonmodified; *blue* = carbonyl formation; *yellow* = oxidation; *green* = dioxidation; and *red* = trioxidation. UP, urinary protein.

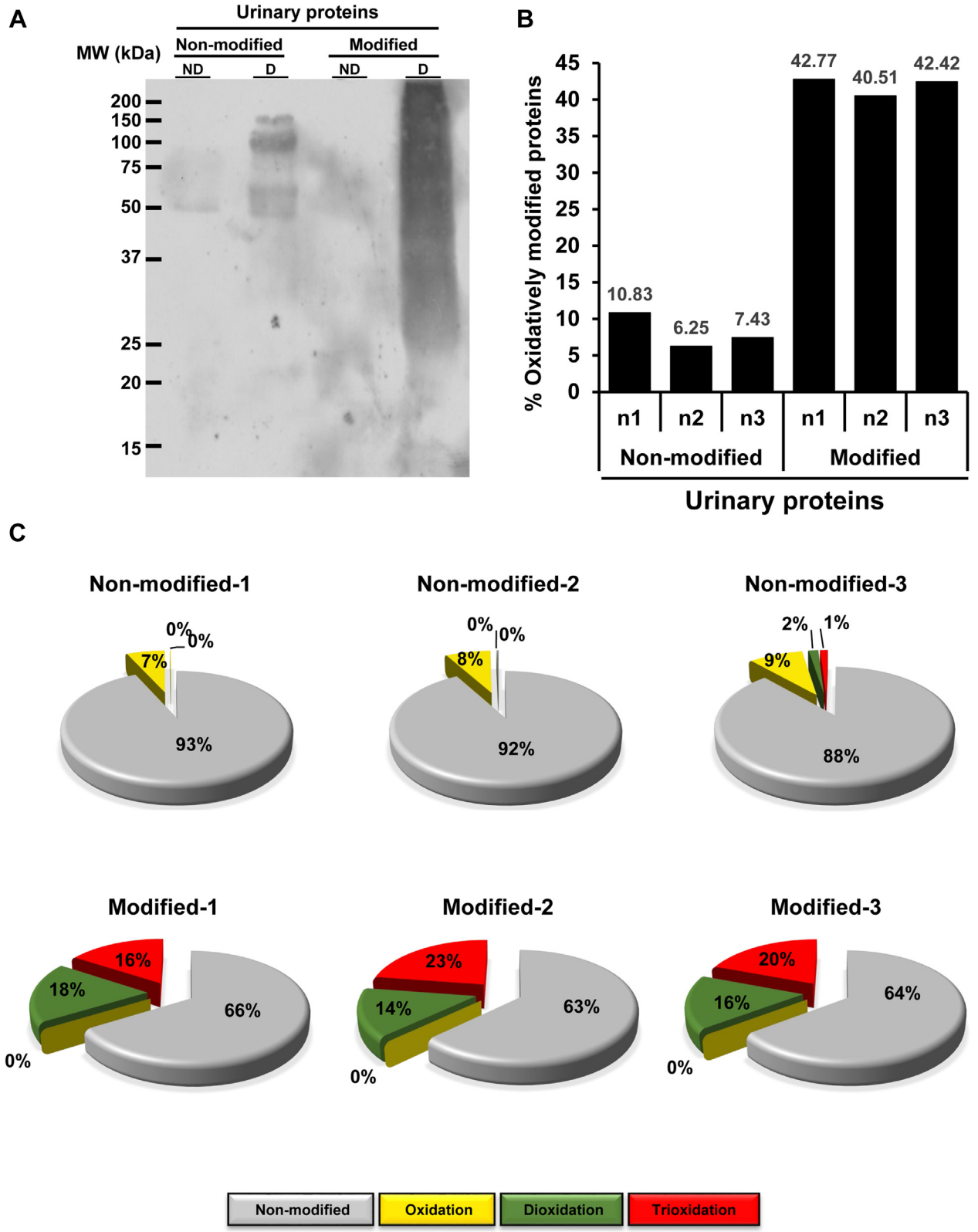

FIG. 2. **Validation of oxidatively modified urinary proteins.** *A*, oxyblot assay was performed to verify the additional carbonyl groups in the performic-modified urinary proteins (ND = nonderivatized [negative control]; D = DNPH derivatized). *B*, percentage of oxidatively modified urinary proteins with the presence of the oxidized residues (including oxidation at methionine, cysteine, or tryptophan; dioxidation at methionine, cysteine, or tryptophan; and trioxidation at cysteine or tryptophan) in the peptides that reached significant identification scores by nanoLC–ESI–LTQ-Orbitrap–MS/MS analysis in each biological replicate. *C*, percentage of the unambiguous oxidatively modified urinary peptides with any of the mentioned oxidized residues found in any peptides from each biological replicate regardless of their identification scores (see also Table 1). *Gray* = nonmodified; *yellow* = oxidation; *green* = dioxidation; and *red* = trioxidation. See more details in supplemental Tables S1–S8. DNPH, 2,4-dinitrophenylhydrazine.

TABLE 1
Details of oxidatively modified peptides and residues identified in nonmodified and modified urine samples

Samples	No. of total identified peptides	No. of nonmodified peptides	No. of oxidatively modified peptides								No. of oxidatively modified peptides/no. of total identified peptides (%)
			Oxidation			Dioxidation			Trioxidation		
			Cysteine (C)	Methionine (M)	Tryptophan (W)	Cysteine (C)	Methionine (M)	Tryptophan (W)	Cysteine (C)	Tryptophan (W)	Total
Nonmodified 1	2778	2591	0	181	2	0	1	2	0	1	187	6.73%
Nonmodified 2	2177	2002	0	167	1	0	0	3	0	4	175	8.04%
Nonmodified 3	1512	1334	0	121	14	0	5	19	0	19	178	11.77%
Modified 1	2035	1343	0	0	0	0	349	17	317	9	692	34.00%
Modified 2	1778	1114	0	0	0	0	239	18	392	15	664	37.35%
Modified 3	1726	1113	0	0	0	0	265	11	324	13	613	35.52%

DISCUSSION

Previously, the majority of oxidative stress studies in kidney stone research had explored only cellular response to ROS and subsequent effects, particularly cellular injury and/or inflammation (24). Nevertheless, the direct effects of oxidative stress on kidney stone formation processes, such as crystallization, crystal nucleation, crystal growth, and crystal aggregation, had not been investigated. Our present study reports for the first time the direct effects of oxidative modifications of urinary proteins on CaOx kidney stone formation processes using various *in vitro* assays. We focused our attention on CaOx stone because CaOx is the most common chemical type of kidney stones found worldwide (accounting for approximately 80% of all kidney stones analyzed) (48). Performic oxidation is one of the classical methods used in several previous proteomics studies to simulate the oxidative stress condition by using a mild oxidizing substance (49–51). The other inducers, for example, H_2O_2, provide a high efficacy to oxidize proteins or peptides. However, the physical properties of protein/peptides may be lost, resulting in protein/peptide malfunctions (49, 50). The present study therefore employed the performic oxidation method with careful validation. The oxidatively modified urinary proteins were successfully confirmed by immunodetection and various approaches based on nanoLC–ESI–LTQ-Orbitrap–MS/MS analyses, all of which demonstrated the increased levels of oxidized proteins, peptides, and amino acid side chains in the performic-modified samples.

Oxyblot assay confirms the protein oxidation byproducts by detecting protein carbonyl groups (52). Performic oxidation increases carbonylation of protein-specific side chains (ketone and aldehyde at lysine, arginine, proline, or threonine residues), which are widely applied as the oxidative stress markers (53). In addition, LC–MS/MS analysis can confirm the increase of cysteine, methionine, and/or tryptophan residual oxidation modifications. Our MS/MS analyses revealed that cysteine and methionine were the two major residues being oxidized by performic modification. Cysteine can regulate protein structure and functions through the formation of disulfide bonds, and methionine is the most common amino acid subjected to oxidation in several circumstances (32). It should be noted that cysteine sulfenic acid is a labile and reversible form as it can be transformed to other more stable oxidized forms (54, 55). As such, it is generally thought that cysteine sulfenic acid is rarely found or undetectable in the samples. However, we observed some proportions of cysteine sulfenic acid in both nonmodified and modified urine samples (Fig. 3 and Table 1). Other lines of evidence also support our findings indicating that recent advanced technologies (in our case, the highly sensitive nanoLC–ESI–LTQ-Orbitrap–MS/MS) can detect cysteine sulfenic acid, which plays important roles in redox mechanisms and related pathways (54, 55). Nevertheless, MS2 spectral profiles of the fragmented ions for

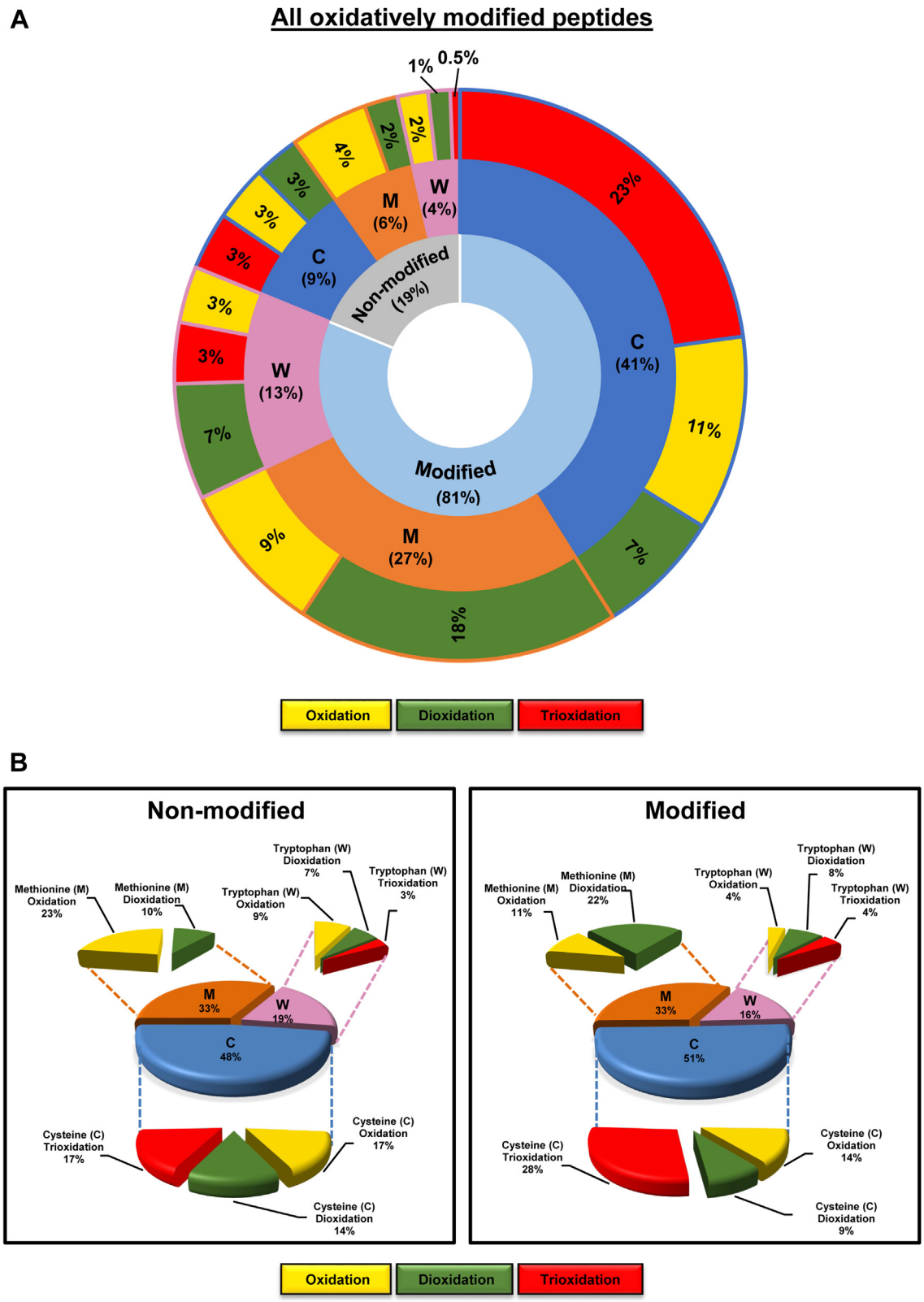

FIG. 3. **Quantitative data of oxidatively modified urinary peptides based on extracted ion chromatograms (XICs).** *A*, a sunburst plot demonstrating the proportion (based on relative spectral intensities) of all oxidatively modified peptides. The *inner layer* demonstrates the proportion of overall oxidatively modified peptides in the nonmodified *versus* performic-modified samples. The *middle layer* shows the proportion of all modified cysteine (C), methionine (M), and tryptophan (W) residues. The *outer layer* indicates individual oxidation forms (including oxidation at C, M, or W; dioxidation at C, M, or W; and trioxidation at C or W) found in the nonmodified and performic-modified urinary proteins. *B*, the percentage of individual oxidative modification forms that were found in all the oxidatively modified peptides identified in nonmodified and modified urine samples. *Yellow* = oxidation; *green* = dioxidation; and *red* = trioxidation.

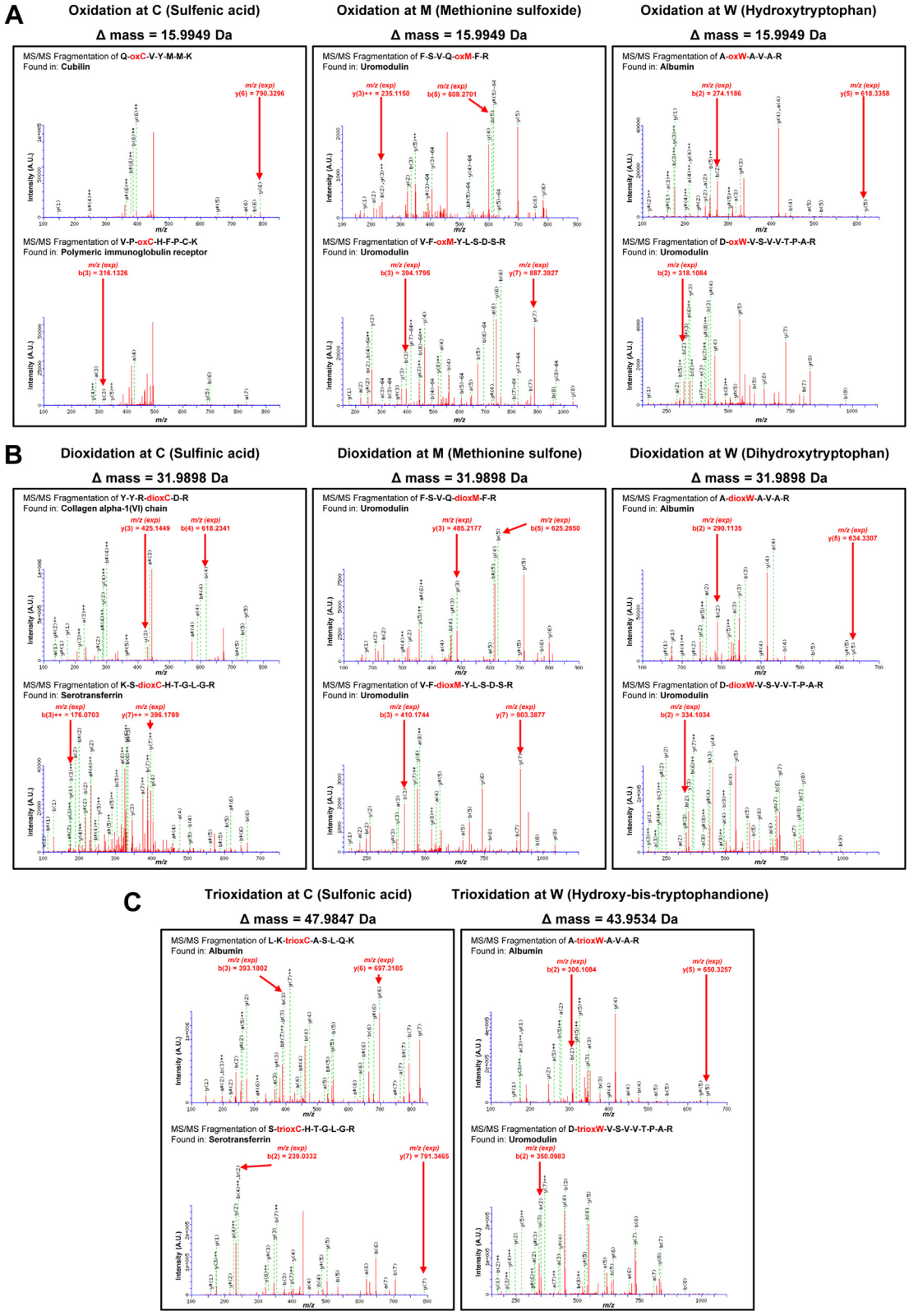

FIG. 4. **Examples of the annotated MS2 spectra of oxidatively modified peptides (two examples for each modification).** *A*, oxidation (sulfenic acid at C, methionine sulfoxide at M, and hydroxytryptophan at W). *B*, dioxidation (sulfinic acid at C, methionine sulfone at M, and dihydroxytryptophan at W). *C*, trioxidation (sulfonic acid at C and hydroxy-bis-tryptophandione at W). The *arrow* indicates the oxidatively modified residue(s).

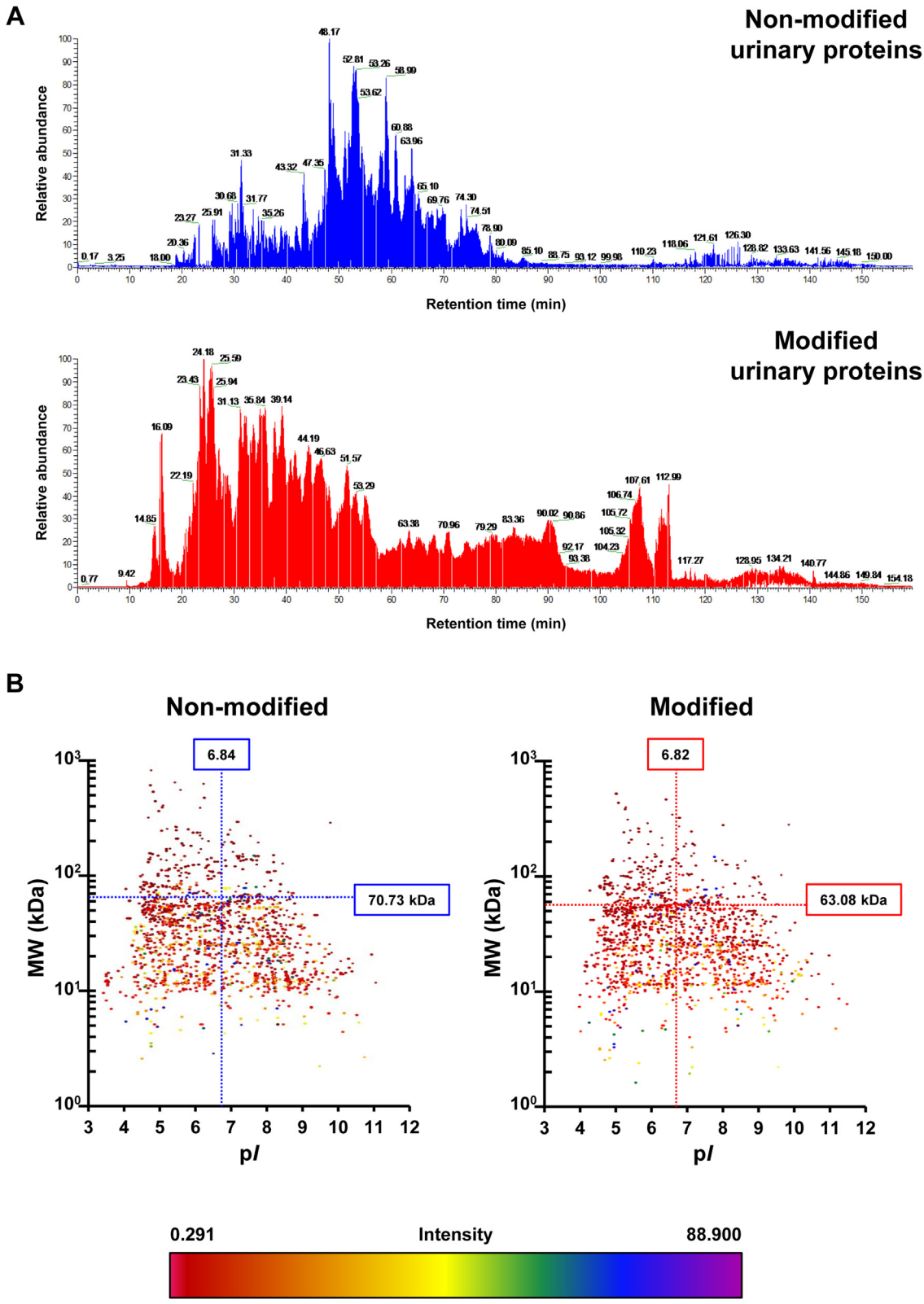

FIG. 5. **Mass spectral pattern of oxidatively modified urinary proteins.** *A*, the 160-min gradient MS chromatograms of nonmodified and performic-modified urinary proteins demonstrated alterations in pattern of relative abundance and retention time. *B*, the distribution of molecular weight (MW) (*y*-axis) and isoelectric point (pI) (*x*-axis) of nonmodified and modified urinary proteins. The indicated values represent average MW and pI in each group.

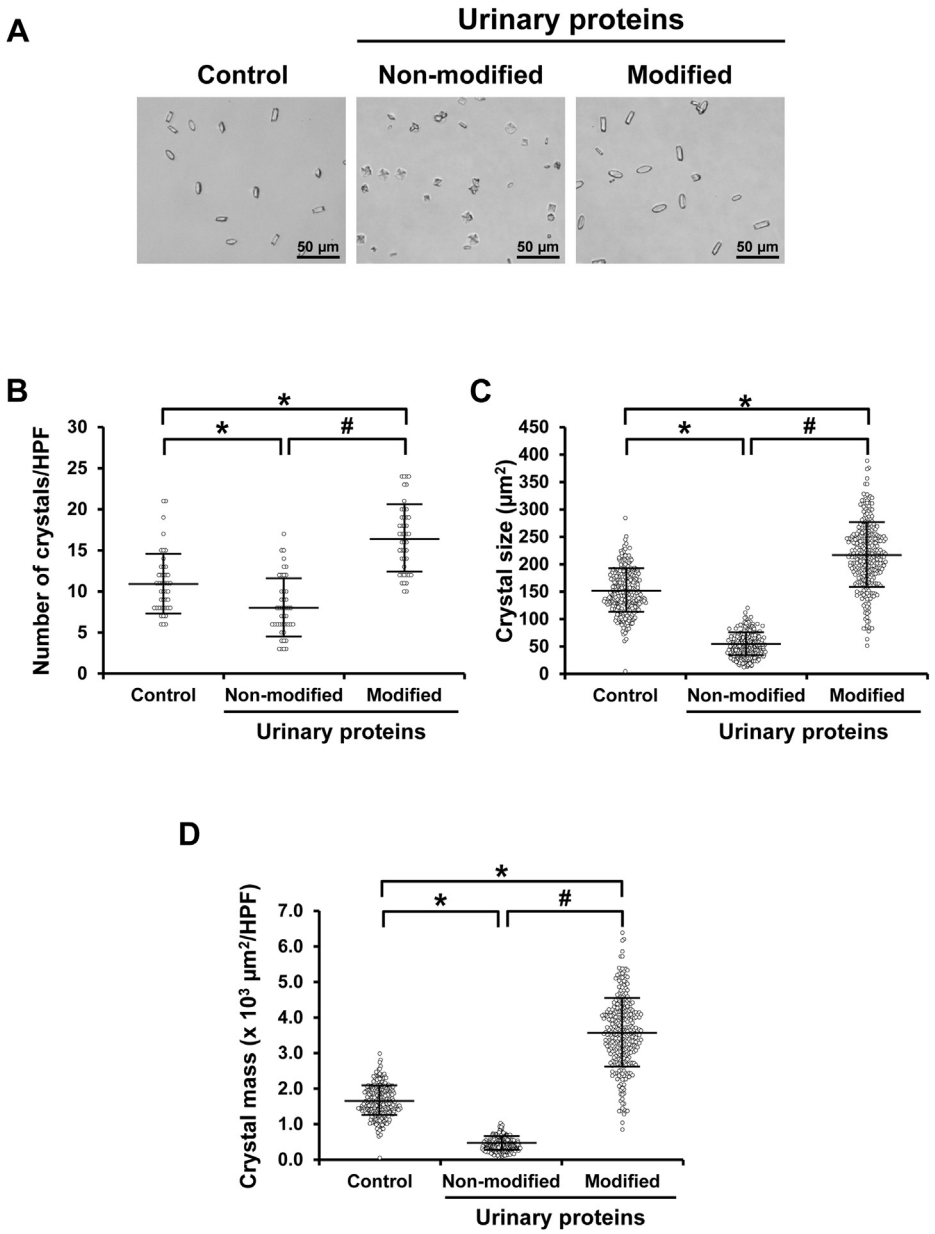

FIG. 6. **Effects of oxidatively modified urinary proteins on CaOx crystallization.** *A*, micrographs of CaOx crystals obtained from the crystallization assay without (control) or with nonmodified or modified urinary proteins. Original magnification was 400× for all panels. Zoom-in images are provided in supplemental Fig. S1. *B*, crystal number was counted from 15 HPFs per well. *C*, crystal size was measured from at least 100 crystals from 15 HPFs per well. *D*, crystal mass was calculated using Equation 1 as detailed in the Experimental Procedures section. The quantitative data are reported as mean ± SD obtained from three biological replicates. $^{*}p < 0.05$ *versus* control; $^{\#}p < 0.05$ *versus* nonmodified urinary proteins. CaOx, calcium oxalate; HPF, high-power field.

cysteine sulfenic acid were not as clear as those for the other modified residues (Fig. 4). Therefore, additional evidence may be required to solidify such detection. Overall, the oxidatively modified urinary proteins generated in our present study had several characteristics that mimic the effects of ROS-induced protein oxidation naturally occurred during oxidative stress condition in the kidney.

These oxidatively modified urinary proteins were used as the main materials for *in vitro* CaOx stone formation assays. Although chemical-induced urinary protein modifications might be more intensely modified than the naturally occurred *in vivo* modifications, it is quite difficult (or perhaps impossible) to explore the direct effects of oxidative modifications of urinary proteins using an *in vivo*

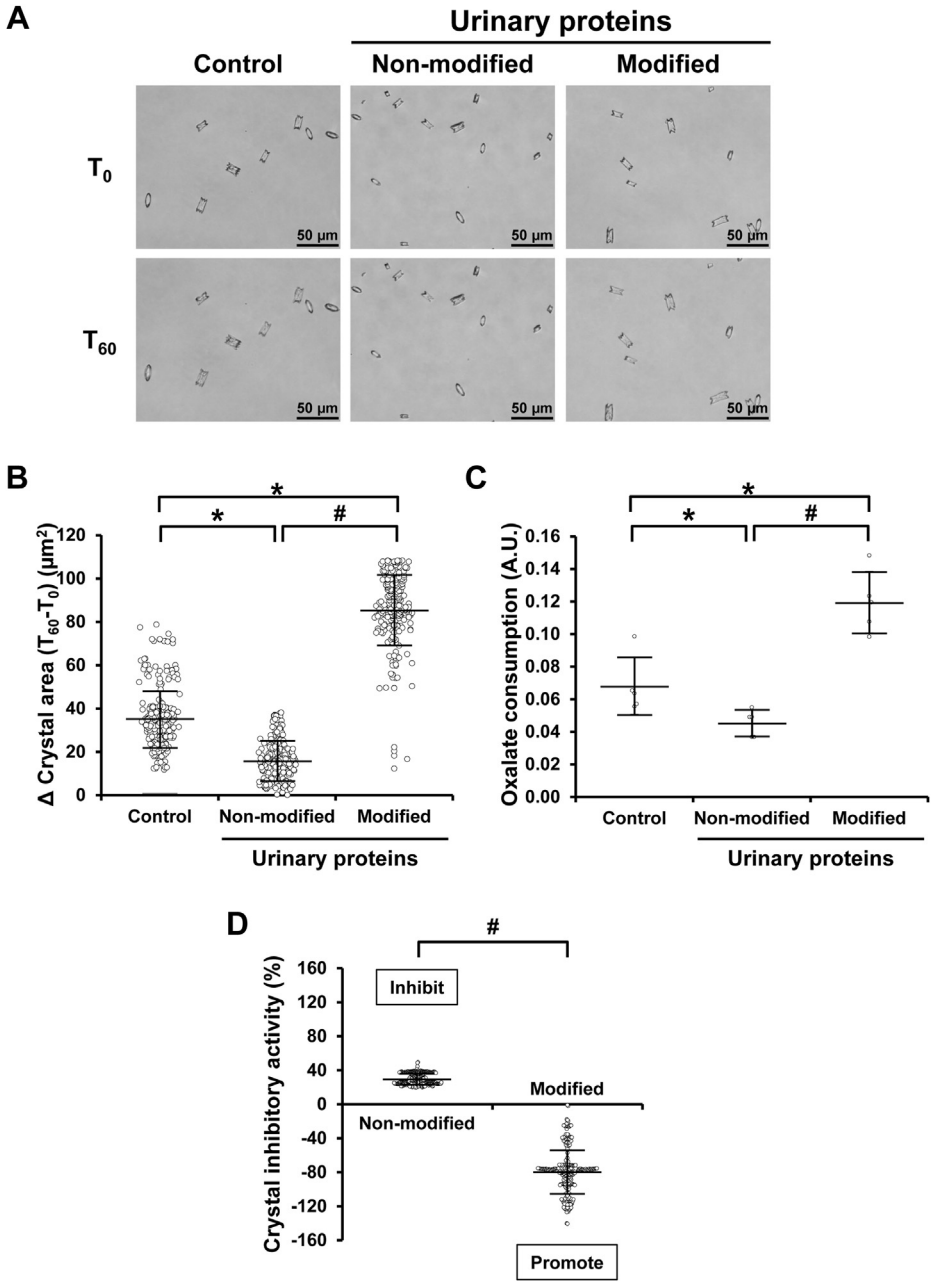

FIG. 7. **Effects of oxidatively modified urinary proteins on CaOx crystal growth.** *A*, micrographs of CaOx crystals obtained from the crystal growth assay (at T_0 and T_{60}) without (control) or with nonmodified or modified urinary proteins. Original magnification was 400× for all panels. Zoom-in images are provided in supplemental Fig. S2. *B*, Δ Crystal area was calculated from 15 HPFs per well using Equation 2 as detailed in the Experimental Procedures section. *C* and *D*, oxalate consumption and inhibitory activity were calculated using Equations 3 and 4, respectively, as detailed in the Experimental Procedures section. The quantitative data are reported as mean ± SD obtained from three biological replicates. $^{*}p < 0.05$ *versus* control; $^{\#}p < 0.05$ *versus* nonmodified urinary proteins. CaOx, calcium oxalate; HPF, high-power field.

model (in either animal or human). This difficulty is mainly because oxidative stress condition has generous effects and affects not only the urinary proteins but also other systems. Moreover, oxidative stress can be the result (effector), not the cause, in various conditions, and there may be certain levels of the background of naturally occurred oxidatively modified proteins in an organ system (that is hard to control). Therefore, using a chemical-induced *in vitro* model to address the effects of oxidative modifications is considerably justified to address the pathogenic roles of oxidatively modified urinary proteins in kidney stone formation processes.

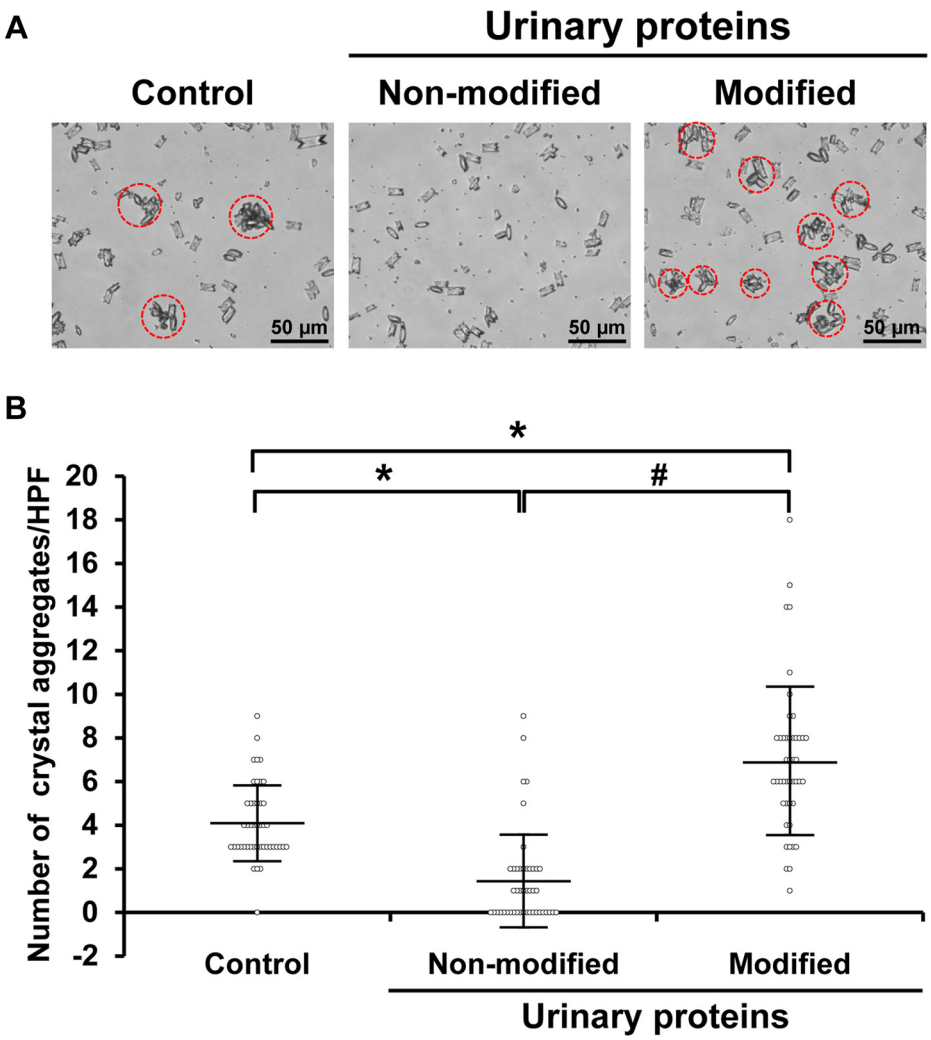

FIG. 8. **Effects of oxidatively modified urinary proteins on CaOx crystal aggregation.** *A*, micrographs of CaOx crystals obtained from the crystal aggregation assay without (control) or with nonmodified or modified urinary proteins. Original magnification was 400× for all panels. *B*, number of CaOx crystal aggregates was counted from 15 random HPFs per well. The *dashed circle* indicates each crystal aggregate, which was defined as an assembly of three or more individual CaOx crystals that tightly joined together. The quantitative data are reported as mean ± SD obtained from three biological replicates. $^{*}p < 0.05$ *versus* control; $^{\#}p < 0.05$ *versus* nonmodified urinary proteins. CaOx, calcium oxalate; HPF, high-power field.

We have demonstrated that the oxidatively modified urinary proteins could promote CaOx crystallization, crystal growth, and aggregation. These studied processes are the important mechanisms for kidney stone formation, particularly in the plug model (1, 2). Please note that these mechanisms may not entirely explain the other model of the stone pathogenesis—the Randall's plaque model, which involves subepithelial deposition of calcium phosphate mineral at renal papillary surface (1, 2). Nevertheless, these studied mechanisms may be partially involved in the latter model, especially after the Randall's plaque forms and erodes into the renal pelvis, where the plaque can serve as the stem or nidus for CaOx deposition and finally stone formation (56–58).

By contrast, the nonmodified urinary proteins inhibited such stone formation mechanisms, consistent with the previous findings demonstrating that the urine from healthy individuals protects the stone nidus formation and retention of CaOx crystals in renal tubular lumens and parenchyma (12, 35, 59). This is the first evidence showing that oxidative stress condition is directly involved in the primary phase of kidney stone formation and is not just the secondary effect from induction of renal tubular cell injury or inflammatory response. The data indicated that oxidative modifications altered the CaOx crystal modulatory activity of urinary proteins. The changes in protein structure and function after carbonyl formation and oxidation of cysteine thiol to sulfenic (Cys-SOH), sulfinic (Cys-SO_2H), and sulfonic (Cys-SO_3H) acids were most likely to be responsible for such alterations in protein–crystal interactions. Especially, sulfonic acid has been reported to bind with calcium ion and CaOx crystals (60, 61). Moreover, methionine

oxidation of immunoglobulin, one of the high-abundance urinary proteins, could increase the protein hydrophilic properties and affinity to cationic surface (62), and tryptophan oxidation could promote immunoglobulin aggregation (63). Therefore, alterations of protein structure and ionic charge could also unveil the calcium- and/or oxalate-binding sites and enhance the crystal–protein complex formation that would enhance the stone nidus formation.

In summary, we report herein the first direct evidence demonstrating that oxidative modifications switch the CaOx crystal modulatory activities of urinary proteins from inhibition to promotion of the stone formation processes, including CaOx crystallization, crystal growth, and crystal aggregation. Therefore, oxidative modifications of urinary proteins increase the risk of kidney stone formation.

DATA AVAILABILITY

The MS proteomics data have been deposited to the ProteomeXchange Consortium (http://www.proteomexchange.org/) *via* the PRIDE (https://www.ebi.ac.uk/pride/) partner repository with the data set identifier PXD019360 and 10.6019/PXD019360.

Supplemental data—This article contains supplemental data.

Acknowledgments—This study was supported by the Mahidol University.

Funding and additional information—V. T. is supported by "Chalermphrakiat" and "Research Staff" grants from the Faculty of Medicine Siriraj Hospital.

Author contributions—S. C. and V. T. conceptualization; S. C. and V. T. methodology; S. C. and V. T. software; S. C. and V. T. validation; S. C. formal analysis; S. C. investigation; V. T. resources; S. C. data curation; S. C. writing–original draft; V. T. writing–review and editing; S. C. visualization; V. T. supervision; V. T. project administration; V. T. funding acquisition.

Conflict of interest—The authors declare no competing interests.

Abbreviations—The abbreviations used are: CaOx, calcium oxalate; ESI, electrospray ionization; HPF, high-power field; LTQ, linear trap quadrupole; ROS, reactive oxygen species.

Received April 21, 2021, and in revised from, September 15, 2021
Published, MCPRO Papers in Press, September 23, 2021, https://doi.org/10.1016/j.mcpro.2021.100151

REFERENCES

1. Khan, S. R., Pearle, M. S., Robertson, W. G., Gambaro, G., Canales, B. K., Doizi, S., Traxer, O., and Tiselius, H. G. (2016) Kidney stones. *Nat. Rev. Dis. Primers* **2**, 16008
2. Khan, A. (2018) Prevalence, pathophysiological mechanisms and factors affecting urolithiasis. *Int. Urol. Nephrol.* **50**, 799–806
3. Marengo, S. R., Chen, D. H., Kaung, H. L., Resnick, M. I., and Yang, L. (2002) Decreased renal expression of the putative calcium oxalate inhibitor Tamm-Horsfall protein in the ethylene glycol rat model of calcium oxalate urolithiasis. *J. Urol.* **167**, 2192–2197
4. Zhang, L., Fujii, S., and Kosaka, H. (2007) Effect of oestrogen on reactive oxygen species production in the aortas of ovariectomized Dahl salt-sensitive rats. *J. Hypertens.* **25**, 407–414
5. Rodgers, A. L., Mensah, P. D., Schwager, S. L., and Sturrock, E. D. (2006) Inhibition of calcium oxalate crystallization by commercial human serum albumin and human urinary albumin isolated from two different race groups: Evidence for possible molecular differences. *Urol. Res.* **34**, 373–380
6. Cerini, C., Geider, S., Dussol, B., Hennequin, C., Daudon, M., Veesler, S., Nitsche, S., Boistelle, R., Berthezene, P., Dupuy, P., Vazi, A., Berland, Y., Dagorn, J. C., and Verdier, J. M. (1999) Nucleation of calcium oxalate crystals by albumin: Involvement in the prevention of stone formation. *Kidney Int.* **55**, 1776–1786
7. Asplin, J., DeGanello, S., Nakagawa, Y. N., and Coe, F. L. (1991) Evidence that nephrocalcin and urine inhibit nucleation of calcium oxalate monohydrate crystals. *Am. J. Physiol.* **261**, F824–F830
8. Grover, P. K., and Ryall, R. L. (2002) Effect of prothrombin and its activation fragments on calcium oxalate crystal growth and aggregation in undiluted human urine *in vitro*: Relationship between protein structure and inhibitory activity. *Clin. Sci. (Lond.)* **102**, 425–434
9. Okuyama, M., Yamaguchi, S., and Yachiku, S. (2003) Identification of bikunin isolated from human urine inhibits calcium oxalate crystal growth and its localization in the kidneys. *Int. J. Urol.* **10**, 530–535
10. Ebisuno, S., Nishihata, M., Inagaki, T., Umehara, M., and Kohjimoto, Y. (1999) Bikunin prevents adhesion of calcium oxalate crystal to renal tubular cells in human urine. *J. Am. Soc. Nephrol.* **10 Suppl 14**, S436–S440
11. Atmani, F., and Khan, S. R. (1999) Role of urinary bikunin in the inhibition of calcium oxalate crystallization. *J. Am. Soc. Nephrol.* **10 Suppl 14**, S385–S388
12. Chutipongtanate, S., Nakagawa, Y., Sritippayawan, S., Pittayamateekul, J., Parichatikanond, P., Westley, B. R., May, F. E., Malasit, P., and Thongboonkerd, V. (2005) Identification of human urinary trefoil factor 1 as a novel calcium oxalate crystal growth inhibitor. *J. Clin. Invest.* **115**, 3613–3622
13. Thongboonkerd, V., Chutipongtanate, S., Semangoen, T., and Malasit, P. (2008) Urinary trefoil factor 1 is a novel potent inhibitor of calcium oxalate crystal growth and aggregation. *J. Urol.* **179**, 1615–1619
14. Khamchun, S., Sueksakit, K., Chaiyarit, S., and Thongboonkerd, V. (2019) Modulatory effects of fibronectin on calcium oxalate crystallization, growth, aggregation, adhesion on renal tubular cells, and invasion through extracellular matrix. *J. Biol. Inorg. Chem.* **24**, 235–246
15. Ceban, E., Banov, P., Galescu, A., and Botnari, V. (2016) Oxidative stress and antioxidant status in patients with complicated urolithiasis. *J. Med. Life* **9**, 259–262
16. Tracy, C. R., Henning, J. R., Newton, M. R., Aviram, M., and Bridget Zimmerman, M. (2014) Oxidative stress and nephrolithiasis: A comparative pilot study evaluating the effect of pomegranate extract on stone risk factors and elevated oxidative stress levels of recurrent stone formers and controls. *Urolithiasis* **42**, 401–408
17. Davalos, M., Konno, S., Eshghi, M., and Choudhury, M. (2010) Oxidative renal cell injury induced by calcium oxalate crystal and renoprotection with antioxidants: A possible role of oxidative stress in nephrolithiasis. *J. Endourol.* **24**, 339–345
18. Hirose, M., Yasui, T., Okada, A., Hamamoto, S., Shimizu, H., Itoh, Y., Tozawa, K., and Kohri, K. (2010) Renal tubular epithelial cell injury and oxidative stress induce calcium oxalate crystal formation in mouse kidney. *Int. J. Urol.* **17**, 83–92
19. Khan, S. R. (2013) Reactive oxygen species as the molecular modulators of calcium oxalate kidney stone formation: Evidence from clinical and experimental investigations. *J. Urol.* **189**, 803–811
20. Kohjimoto, Y., Ebisuno, S., Tamura, M., and Ohkawa, T. (1996) Interactions between calcium oxalate monohydrate crystals and Madin-Darby canine kidney cells: Endocytosis and cell proliferation. *Urol. Res.* **24**, 193–199
21. Thongboonkerd, V., Semangoen, T., Sinchaikul, S., and Chen, S. T. (2008) Proteomic analysis of calcium oxalate monohydrate crystal-induced cytotoxicity in distal renal tubular cells. *J. Proteome. Res.* **7**, 4689–4700

22. Peerapen, P., and Thongboonkerd, V. (2011) Effects of calcium oxalate monohydrate crystals on expression and function of tight junction of renal tubular epithelial cells. *Lab. Invest.* **91**, 97–105
23. Chaiyarit, S., and Thongboonkerd, V. (2012) Changes in mitochondrial proteome of renal tubular cells induced by calcium oxalate monohydrate crystal adhesion and internalization are related to mitochondrial dysfunction. *J. Proteome. Res.* **11**, 3269–3280
24. Khan, S. R. (2014) Reactive oxygen species, inflammation and calcium oxalate nephrolithiasis. *Transl. Androl. Urol.* **3**, 256–276
25. Thongboonkerd, V. (2019) Proteomics of crystal-cell interactions: A model for kidney stone research. *Cells* **8**, 1076
26. Wang, Y., Sun, C., Li, C., Deng, Y., Zeng, G., Tao, Z., Wang, X., Guan, X., and Zhao, Y. (2017) Urinary MCP-1HMGB1 increased in calcium nephrolithiasis patients and the influence of hypercalciuria on the production of the two cytokines. *Urolithiasis* **45**, 159–175
27. Khan, S. R. (2005) Hyperoxaluria-induced oxidative stress and antioxidants for renal protection. *Urol. Res.* **33**, 349–357
28. Halliwell, B., and Whiteman, M. (2004) Measuring reactive species and oxidative damage *in vivo* and in cell culture: How should you do it and what do the results mean? *Br. J. Pharmacol.* **142**, 231–255
29. Hopps, E., and Caimi, G. (2013) Protein oxidation in metabolic syndrome. *Clin. Invest. Med.* **36**, E1–E8
30. Garcia-Garcia, A., Rodriguez-Rocha, H., Madayiputhiya, N., Pappa, A., Panayiotidis, M. I., and Franco, R. (2012) Biomarkers of protein oxidation in human disease. *Curr. Mol. Med.* **12**, 681–697
31. Ahmad, S., Khan, H., Shahab, U., Rehman, S., Rafi, Z., Khan, M. Y., Ansari, A., Siddiqui, Z., Ashraf, J. M., Abdullah, S. M., Habib, S., and Uddin, M. (2017) Protein oxidation: An overview of metabolism of sulphur containing amino acid, cysteine. *Front. Biosci. (Schol. Ed.)* **9**, 71–87
32. Barelli, S., Canellini, G., Thadikkaran, L., Crettaz, D., Quadroni, M., Rossier, J. S., Tissot, J. D., and Lion, N. (2008) Oxidation of proteins: Basic principles and perspectives for blood proteomics. *Proteomics Clin. Appl.* **2**, 142–157
33. Aggarwal, K. P., Tandon, S., Naik, P. K., Singh, S. K., and Tandon, C. (2013) Peeping into human renal calcium oxalate stone matrix: Characterization of novel proteins involved in the intricate mechanism of urolithiasis. *PLoS One* **8**, e69916
34. Kumar, V., Pena de la Vega, L., Farell, G., and Lieske, J. C. (2005) Urinary macromolecular inhibition of crystal adhesion to renal epithelial cells is impaired in male stone formers. *Kidney Int.* **68**, 1784–1792
35. Aggarwal, S., Tandon, C., Forouzandeh, M., Singla, S. K., Kiran, R., and Jethi, R. K. (2005) Role of a protein inhibitor isolated from human renal stone matrix in urolithiasis. *Indian J. Biochem. Biophys.* **42**, 113–117
36. Aluksanasuwan, S., Sueksakit, K., Fong-Ngern, K., and Thongboonkerd, V. (2017) Role of HSP60 (HSPD1) in diabetes-induced renal tubular dysfunction: Regulation of intracellular protein aggregation, ATP production, and oxidative stress. *FASEB J.* **31**, 2157–2167
37. Vinaiphat, A., Aluksanasuwan, S., Manissorn, J., Sutthimethakorn, S., and Thongboonkerd, V. (2017) Response of renal tubular cells to differential types and doses of calcium oxalate crystals: Integrative proteome network analysis and functional investigations. *Proteomics* **17**, 1700192
38. Chanthick, C., and Thongboonkerd, V. (2019) Cellular proteome datasets of human endothelial cells under physiologic state and after treatment with caffeine and epigallocatechin-3-gallate. *Data Brief* **25**, 104292
39. Chanthick, C., and Thongboonkerd, V. (2019) Comparative proteomics reveals concordant and discordant biochemical effects of caffeine versus epigallocatechin-3-gallate in human endothelial cells. *Toxicol. Appl. Pharmacol.* **378**, 114621
40. Vinaiphat, A., Charngkaew, K., and Thongboonkerd, V. (2018) More complete polarization of renal tubular epithelial cells by artificial urine. *Cell Death Discov.* **5**, 47
41. Manissorn, J., Fong-ngern, K., Peerapen, P., and Thongboonkerd, V. (2017) Systematic evaluation for effects of urine pH on calcium oxalate crystallization, crystal-cell adhesion and internalization into renal tubular cells. *Sci. Rep.* **7**, 1798
42. Thongboonkerd, V., Semangoen, T., and Chutipongtanate, S. (2006) Factors determining types and morphologies of calcium oxalate crystals: Molar concentrations, buffering, pH, stirring and temperature. *Clin. Chim. Acta* **367**, 120–131
43. Peerapen, P., and Thongboonkerd, V. (2016) Caffeine prevents kidney stone formation by translocation of apical surface annexin A1 crystal-binding protein into cytoplasm: *In vitro* evidence. *Sci. Rep.* **6**, 38536
44. Sueksakit, K., and Thongboonkerd, V. (2019) Protective effects of finasteride against testosterone-induced calcium oxalate crystallization and crystal-cell adhesion. *J Biol. Inorg. Chem.* **24**, 973–983
45. Chutipongtanate, S., and Thongboonkerd, V. (2010) Red blood cell membrane fragments but not intact red blood cells promote calcium oxalate monohydrate crystal growth and aggregation. *J. Urol.* **184**, 743–749
46. Chaiyarit, S., and Thongboonkerd, V. (2017) Defining and systematic analyses of aggregation indices to evaluate degree of calcium oxalate crystal aggregation. *Front. Chem.* **5**, 113
47. Kanlaya, R., Naruepantawart, O., and Thongboonkerd, V. (2019) Flagellum is responsible for promoting effects of viable *Escherichia coli* on calcium oxalate crystallization, crystal growth, and crystal aggregation. *Front. Microbiol.* **10**, 2507
48. Schubert, G. (2006) Stone analysis. *Urol. Res.* **34**, 146–150
49. Pesavento, J. J., Garcia, B. A., Streeky, J. A., Kelleher, N. L., and Mizzen, C. A. (2007) Mild performic acid oxidation enhances chromatographic and top down mass spectrometric analyses of histones. *Mol. Cell. Proteomics* **6**, 1510–1526
50. Simpson, R. J. (2007) Performic acid oxidation of proteins. *CSH Protoc.* **2007**. pdb.prot4698
51. Matthiesen, R., Bauw, G., and Welinder, K. G. (2004) Use of performic acid oxidation to expand the mass distribution of tryptic peptides. *Anal. Chem.* **76**, 6848–6852
52. Robinson, C. E., Keshavarzian, A., Pasco, D. S., Frommel, T. O., Winship, D. H., and Holmes, E. W. (1999) Determination of protein carbonyl groups by immunoblotting. *Anal. Biochem.* **266**, 48–57
53. Dalle-Donne, I., Rossi, R., Colombo, R., Giustarini, D., and Milzani, A. (2006) Biomarkers of oxidative damage in human disease. *Clin. Chem.* **52**, 601–623
54. Gupta, V., and Carroll, K. S. (2014) Sulfenic acid chemistry, detection and cellular lifetime. *Biochim. Biophys. Acta* **1840**, 847–875
55. Verrastro, I., Pasha, S., Jensen, K. T., Pitt, A. R., and Spickett, C. M. (2015) Mass spectrometry-based methods for identifying oxidized proteins in disease: Advances and challenges. *Biomolecules* **5**, 378–411
56. Khan, S. R., Canales, B. K., and Dominguez-Gutierrez, P. R. (2021) Randall's plaque and calcium oxalate stone formation: Role for immunity and inflammation. *Nat. Rev. Nephrol.* **17**, 417–433
57. Chaiyarit, S., and Thongboonkerd, V. (2020) Mitochondrial dysfunction and kidney stone disease. *Front. Physiol.* **11**, 566506
58. Wiener, S. V., Ho, S. P., and Stoller, M. L. (2018) Beginnings of nephrolithiasis: Insights into the past, present and future of Randall's plaque formation research. *Curr. Opin. Nephrol. Hypertens.* **27**, 236–242
59. Moghadam, M. F., Tandon, C., Aggarwal, S., Singla, S. K., Singh, S. K., Sharma, S. K., Varshney, G. C., and Jethi, R. K. (2003) Concentration of a potent calcium oxalate monohydrate crystal growth inhibitor in the urine of normal persons and kidney stone patients by ELISA-based assay system employing monoclonal antibodies. *J. Cell. Biochem.* **90**, 1261–1275
60. Luo, J., Ma, Z., Liang, H., Chen, J., and Zeng, Z. (2012) K, Ca complexes with a sulfonic ligand: Structure and DNA-binding properties. *Spectrochim. Acta A Mol. Biomol. Spectrosc.* **90**, 202–207
61. Kirboga, S., and Oner, M. (2010) The role of vinyl sulfonic acid homopolymer in calcium oxalate crystallization. *Colloids Surf. B Biointerfaces* **78**, 357–362
62. Bozic, B., Cucnik, S., Kveder, T., and Rozman, B. (2006) Changes in avidity and specificity of IgG during electro-oxidation. Relevance of binding of antibodies to beta2-GPI. *Autoimmun. Rev.* **6**, 28–32
63. Alam, M. E., Slaney, T. R., Wu, L., Das, T. K., Kar, S., Barnett, G. V., Leone, A., and Tessier, P. M. (2020) Unique impacts of methionine oxidation, tryptophan oxidation, and asparagine deamidation on antibody stability and aggregation. *J. Pharm. Sci.* **109**, 656–669